

PLANAR MEMS SUPERCAPACITOR USING CARBON NANOTUBE FORESTS

Y.Q. Jiang, Q. Zhou, and L. Lin

Mechanical Engineering Department, Berkeley Sensor and Actuator Center
University of California, Berkeley CA 94720, USA

ABSTRACT

Planar micro supercapacitors utilizing vertically aligned carbon nanotube (CNT) forests with the design of interdigital electrodes have been demonstrated. Conductive substrates using Mo/Al/Fe metal stack shows best CNT forest synthesis results with high electrical conductivity and dense CNT structures. Prototype devices show measured specific capacitances about 1000 times higher than those with plain metal electrodes without CNT forests. Furthermore, charging/discharging experiments show over 92% efficiency and very robust cycling stability. As such, we believe these planar MEMS supercapacitors could be applicable in various systems including energy harvesters, pulse-power supplies and advanced microelectronics as on-chip capacitors.

INTRODUCTION

A supercapacitor is a charge storage device composed of two electrodes with electrolyte in between. There are two fundamental differences between a supercapacitor and a regular capacitor: First, ion-conducting electrolyte is used in the supercapacitor instead of dielectrics. As a result, under a biased voltage, the positive and negative ions in electrolyte will separate, migrate and accumulate around the electrode surface, forming a nm-thin layer called electro-chemical double layer (EDL). Therefore, there are essentially two EDL capacitors connected in serial within a single supercapacitor. Second, extremely porous electrode materials are needed in supercapacitors to enhance the interfacial capacitance. Porous electrodes maximize the EDL phenomenon and give supercapacitors an astonishingly high value of specific capacitance (capacitance per unit area). Furthermore, unlike fuel cells and Li-ion batteries, supercapacitors require no chemical reaction during its charging/ discharging process to rapidly store/release energy, making it a popular candidate in applications like vehicle regenerative braking and camera flash systems.

In the field of MEMS, supercapacitors could find very promising applications. For example, as a power source without involving chemical reactions, supercapacitors are ideally suited for the energy suppliers in pulse-power applications such as solid-state sensors. Supercapacitors have simple configuration, stable performance (millions cycles vs. ~ 1000 cycles of Li-ion batteries [1]), and less temperature dependency, making them suitable as the main power sources for short-term, high power-density usages in many applications. Moreover, one might envision that supercapacitor can temporarily store energy from energy harvester and power the system for sensing and wireless communication needs. We also believe that the demonstration of the capability of “planar” structure for supercapacitors could inspire new architecture in circuit designs such as on-chip supercapacitors for advanced microelectronics.

The concept of “planar supercapacitor” has been investigated sparsely previously. For example, Sung et al. have used conducting polymer-coated metal layer [2] as planar electrodes to make supercapacitors. However, their electrodes have rather flat metal surface as essentially 2-D structure without the highly porous characteristics. In another work, In et al used KOH etching to increase the surface area [3]. Carbon nanotubes (CNT) are well-known for its high surface area-to-volume ratio and good conductivity such that several groups have used them in large-scale supercapacitors. For example, An et al. have deposited random CNT network as electrodes [4], in which contact resistance among tubes as well as contact to the substrate are major technical challenges. Pushparaj et al. have proposed and demonstrated a complicated process by transferring CNT arrays to a conductive substrate after the synthesis process while no CNT-based planar architecture has been proposed [5].

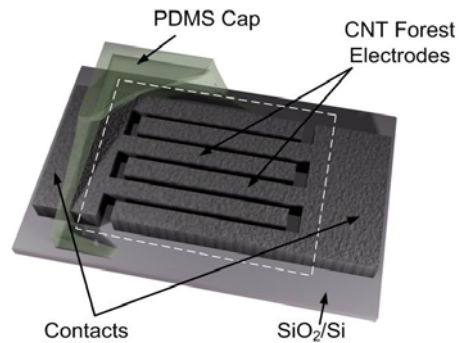


Figure 1: Schematic of the planar micro supercapacitor using aligned, 3D CNT forest electrodes.

Here we present a simple, yet versatile planar MEMS supercapacitor using porous CNT forests as electrodes with low contact resistance without using the top/bottom electrode architecture. The goal of our research is to demonstrate on-chip supercapacitor that can be integrated with MEMS devices and CMOS in a single chip. Figure 1 shows the schematic diagram of a planar supercapacitor with a top cap to contain electrolyte. Unlike the conventional sandwich structure, the two electrodes are made on the same plane. The major advantages of this design include size reduction and simplification of fabrication process such as sophisticated bonding. Furthermore, the travelling distance of ions in the electrolyte, a major performance factor in supercapacitors, can be well controlled and shortened while eliminating the necessity of a separator, which is indispensable in the sandwich-type supercapacitors to prevent electrical short.

CNTS ON CONDUCTIVE SUBSTRATE

Activated carbon (AC) has been widely used as the

electrode materials for supercapacitors currently in use. It could have a very large surface area ($\sim 1200 \text{ m}^2/\text{g}$ [6]) but the major drawback of AC is its pore distribution. There are three classes of pores in AC: micropore ($D < 2\text{nm}$), mesopore ($2\text{nm} < D < 50\text{nm}$), and macropore ($50\text{nm} < D$) [1, 6]. Micropores can significantly increase surface area but fail to produce the effect of double-layer capacitance due to the difficulties of ion diffusion and ion-sieving effect [1, 6]. AC also has high internal resistance caused by its low conductivity ($\sim 2.5\text{S}/\text{cm}$) and numerous contacts between AC particles. CNTs, on the other hand, have a moderate surface area ($100\text{-}500\text{m}^2/\text{g}$ [7]), however, most of them are mesopores having double-layer contribution [8] with excellent conductivity ($100\text{S}/\text{cm}$ [9]). Furthermore, each tube is individually connected to the substrate to lower the internal/contact resistance. The construction of CNT forests can be binder-free thanks to van der Waals force among them. Compared to powered AC, the much better structured pores help facilitating the transfer of electrolyte ions, resulting in rapid rate capability [8].

One major challenge in CNT-based MEMS supercapacitor is the choice of substrate as it plays two important roles: 1) a back layer suitable for the synthesis of CNTs and 2) a low-resistance current collector. Considering the fact that CNTs grow predominantly on non-conducting substrates [10], we carried out extensive experiments to investigate the quality of CNT and their contact resistance to the substrate. Thermally oxidized silicon wafers were used as the common insulating substrate and iron as the common catalyst with results summarized in Table 1. Resistances were measured with a pair of probes on the samples of same size with a constant distance. Some trends are observed based on limited results. We observed two opposite extremes: aluminum (Al) and molybdenum (Mo) are representative examples. Al is a well-known metal suitable for CNT growth. We were able to grow thick and dense aligned CNT array on the Al layer. However, although the Al layer initially exhibited low resistance of about 10Ω , the resistance jumped to $16\text{k}\Omega$ at the end of the synthesis process. One possible explanation is that, under high temperature synthesis, Al may react with the carbon source, forming an insulating AlC layer. Contrarily, the resistance of Mo layer reduced from $\sim 200\Omega$ to 40Ω after the synthesis process, probably due to thermal annealing process during the CNT synthesis. Unfortunately, the problem comes that Mo is not adequate for the growth of CNTs since we hardly found CNT growth using the Mo layer under Scanning electron microscope (SEM). Other metal layers showed more or less intermediate characteristics, either close to Al or to Mo, but none showed the combined

advantages of the two extremes: thriving CNTs and low contact resistance. We proposed and, after numerous tests, experimentally verified the concept of metal stack method to solve such dilemma. It is found the combination of Mo/Al layer gives very satisfactory results. We hypothesize that the insertion of Al layer prohibits the alloying of Mo and Fe, which would otherwise make Fe lose its catalytic activities on the formation of CNTs. Meanwhile, the alloying of Mo and Al somehow avoid the formation of AlC, leaving native Al_2O_3 a well-known material for the growth of CNT on the top. It should be pointed out that we also got similar success on the recipe of W/Al stack layer, demonstrating that this methodology can be a general methodology. Further study should be carried out to investigate whether Al or native Al_2O_3 layer plays the major role in this methodology and why Al_2O_3 or AlC does not affect the contact resistance as people intuitively would expect.

Figure 2 shows vertically aligned multiwalled CNTs synthesized on the lithography-patterned Mo/Al substrate. The width/gap of the porous CNT electrodes was $40\mu\text{m}/20\mu\text{m}$ in (a) and (b) and $60\mu\text{m}/30\mu\text{m}$ in (c) and (d) all with a uniform height of about $80\mu\text{m}$. A close view in Figure 2(d) shows that, while each individual CNT is directly connected to the substrate, and minimizing the contact resistance, the “dense” forests are actually highly porous for the diffusion of electrolyte, forming a real 3-D conductive network.

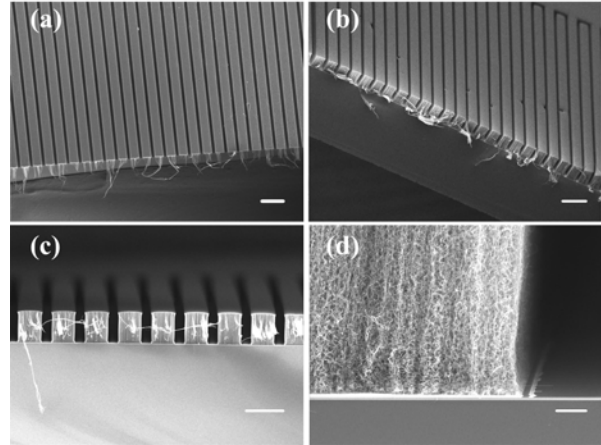


Figure 2: SEM pictures of interdigital CNT electrodes grown on the Mo/Al/Fe stack layer. (a) top view; (b) oblique view; (c) cross-section view; and (d) close view of the contact region. All the bars except (d) are $100\mu\text{m}$. The bar in (d) is $4\mu\text{m}$.

Metal type	Ti (50)	Cr (50)	Ni (50)	Al (50)	Mo (50)	Mo/Al (50nm/10nm)
Resistance before growth, R1	145	140	21	7.5	233	216
Resistance after growth, R2	11.7k	49.6k	373	16.7k	40	26
Ratio of R2/R1	>80	>354	>17	>15560	-0.17	-0.12
CNT profile	Short and sparse	Long but sparse	Hardly any	Thick and dense	No at all	Thick and dense
SEM pictures						

Table 1: CNT syntheses on different metal layers. The number in the brackets is the thickness (unit: nm). The resistance unit is ohm. The synthesis parameters were exactly the same. The bar in the SEM picture of Ti is $2\mu\text{m}$ and applies to all the other pictures.

FABRICATION

The fabrication process began with thermal oxidation of a bare silicon wafer to isolate the substrate from the electrodes. Then lithography was made to pattern two comb-like interdigital electrodes. After that, Mo, Al, and Fe were evaporated onto the substrate with a thickness of 50nm, 10nm, and 5nm, respectively. Fe acts as the common catalyst of CNT growth in this paper. A photoresist lift-off followed to remove the metals on unwanted areas. Thermal chemical vapor deposition (CVD) furnace (Lindberg/Blue M[®] three-zone tube furnace, Thermo Electron Corp., Asheville, NC) was used to grow the CNTs. The furnace was firstly purged with hydrogen and then heated up to 720°C in hydrogen environment. Subsequently, the mixture of ethylene and hydrogen with a proportion of about 1:3 was flowed through the quartz tube for 10 minutes. Finally the tube was left cooling down to room temperature with the help of a fan. Leading wires were bonded to the CNT electrodes using silver epoxy paste. 1-Butyl-3-methylimidazolium tetrafluoro-borate ([BMIM][BF₄]) ionic liquid (Sigma-Aldrich inc., MO) was used as the electrolyte with a PDMS cap to the chip and limit its flow. The main reason that we chose ionic liquid rather than aqueous electrolyte (such as KOH solution) is its high breakdown voltage (~3V vs. ~1V for aqueous electrolyte).

Figure 3 shows the assembled prototype. The CNT electrode area was 5mm×7mm with about 30 comb fingers on a single electrode. Note that the area can be easily scaled down by simply changing the lithography mask.

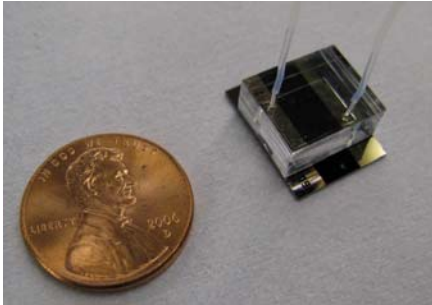


Figure 3: Assembled prototype. A PDMS cap was used to limit the electrolyte within a fixed 5mm×7mm CNT region.

RESULTS AND DISCUSSION

The characterization of the CNT supercapacitor was conducted by the CHI 750A electrochemical workstation (CH Instruments, Inc. USA). Figure 4 shows the cyclic voltammetry curves of supercapacitors using CNT electrodes. As can be seen, our device presents a very symmetric rectangular shape (the ideal supercapacitor should have a perfect rectangular shape). The specific capacitance of our CNT-based supercapacitor can be calculated by:

$$C_{sp} = \frac{I}{dV/dt} \frac{1}{A} \quad (1)$$

Here we represent I with the current at $V=0$; dV/dt was set manually on the equipment as 50mV/sec in Figure 4. A is the effective CNT forest area exposed to electrolyte, 26.7mm² (this value is less than the visible 5mm×7mm area because we exclude the artificial gap area between two electrodes.). Therefore, the capacitance of a single

device was calculated as 149.7μF and specific capacitance as 428μF/cm². As a comparison, we also show the supercapacitor using the identical Mo/Al/Fe electrode but without CNT forests. It is observed that the CV curve with no CNT forests was squeezed into a “straight line”. An enlarged view is shown on the upper left corner. Comparing the current level, the CNT supercapacitor has roughly three orders of magnitude higher than those with only plain metal electrodes. It is noteworthy that this ratio was quite consistent among dozens of samples we tested, firmly contributing this dramatic increase to the benefit of 3D CNT forests. The porosity of 3D CNT forest was also verified by the apogee that, if the CNT forest were solid (no electrolyte could diffuse into the CNT forests), the capacitance should have been increased by only a factor of three due to increases in the sidewall area of the CNT finger electrodes.

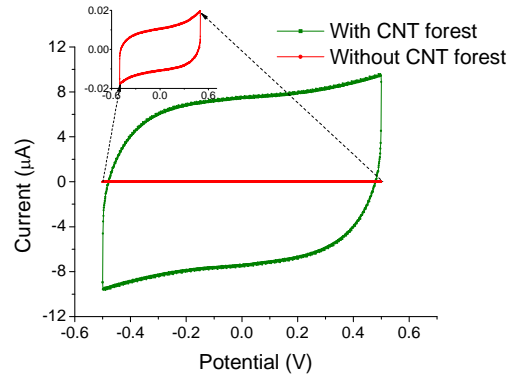


Figure 4: Cyclic voltammetry curves of the samples with (green) and without (red) CNT covering. Scanning rate is 50mV/sec. The inset shows an enlarged view of the curve of bare-metal sample. The units are the same in both coordinates.

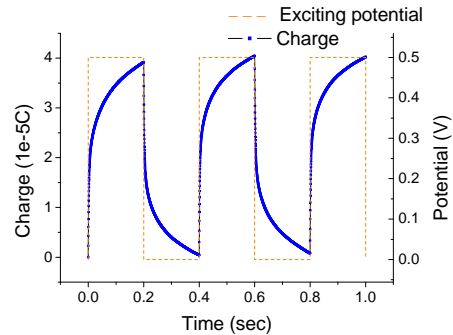


Figure 5: Chronocoulometry curve of the CNT supercapacitor. The device was charged and discharged under a square-wave voltage toggling between 0.5V and 0V at a period of 0.4s.

Figure 5 shows the chronocoulometry curve, presenting the charge/discharge capacity of our device. Defining the charge efficiency as $\Delta Q_{DISCHARGE} / \Delta Q_{CHARGE}$ per cycle, we got an impressively high efficiency of over 92%. This is partly owed to little energy dissipation because of low internal resistance. Under these conditions, an average power density of 0.28mW/cm² was calculated using the equation.

$$\bar{P} = \frac{\Delta Q V_0}{\Delta t} \frac{1}{A} \quad (2)$$

where ΔQ is the charge accumulated during the charge session, Δt is the charge time. V_0 is the constant charge voltage, and again A is the effective carbon forest area. Figure 6 shows the charge efficiency for 10 continuous cycles. As expected, little performance degradation was observed, demonstrating a robust operation, a fundamental superiority of supercapacitors over those chemical reaction-based micro power sources.

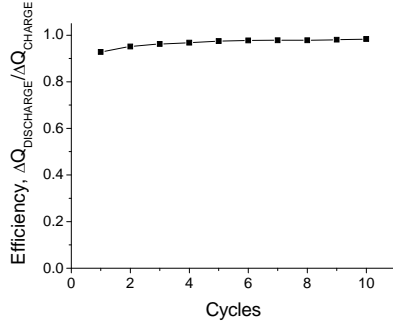


Figure 6: Efficiency variation during 10 continuous charge/discharge cycles. An excellent efficiency of over 92% was observed demonstrating a robust device.

To investigate how well the ionic liquid interacts with CNT forest, we evaluate the theoretical maximum capacitance for our current device. The supercapacitor can be expressed as

$$C = \frac{\epsilon_0 \epsilon_r A}{d} \quad (3)$$

where ϵ_0 is the permittivity of the vacuum, 8.854×10^{-12} F/m. ϵ_r is the relative permittivity of the electrolyte, 11.7 for [BMIM][BF₄] [11]; d is the double-layer thickness, also electrolyte-dependent parameter, 0.69 nm here [12], and A is the overall surface area of electrodes. Because our CNT forests are made of multiwalled carbon nanotubes with a diameter of about 30 nm, we choose 110 m²/g accordingly as an approximation of surface-to-mass ratio [7]. We measured the mass of CNT forests on a device at about 3×10^{-5} g, which then gives a total surface area of 3.3×10^{-3} m². Noticing this value should be divided equally between two electrodes, such that the area in Eq. (3) in the equation should be 1.65×10^{-3} m². Substituting these values into the equation, we get the theoretical peak capacitance for a single device as 248 μ F. Compared to our measured value 149.7 μ F, the utilization of surface area is about 60%. The reason that the CNT forests are not fully employed may be because that there is some air bubble trapped within the interior of CNT forests, blocking electrolyte from accessing part of CNT surface. Slowing down the filling speed of electrolyte to let the air vent and filling the electrolyte within low pressure environment may help to solve this problem.

CONCLUSIONS

We introduced the supercapacitor into micro scale by designing a novel planar MEMS supercapacitor using vertically aligned CNT forest as the electrodes. Unique metal stack layers are proposed as the conductive substrate, which generated both highly ordered CNT forest and low contact resistance. The results show our CNT-covered supercapacitor has generated a specific capacitance of 428 μ F/cm², three orders higher than those merely using

metal electrodes. The samples show an excellent charge efficiency of 92% and a robust cycling stability. We also analyzed the difference between theoretical and measured values and proposed directions in future investigations. We believe MEMS supercapacitors will have promising applications in Microsystem including energy storage, pulse-power supply and on-chip capacitive components. Besides, the methodology of directly synthesize aligned and patterned CNTs using metal stack layers offers a general tool extend the utilization of CNTs in diverse MEMS applications.

ACKNOWLEDGEMENTS

The authors thank Professor Luke P. Lee and John Waldeisen in the department of Bioengineering at UC Berkeley, for generous help in sample measurements. This project is supported in part by the DARPA N/MEMS Fundamentals Program and Siemens Inc..

REFERENCES

- [1] B. E. Conway, *Electrochemical Supercapacitors: Scientific Fundamentals and Technological Applications*, Kluwer Academic/Plenum Publishers, New York, 1999.
- [2] J.H. Sung, S.J. Kim, and K.H. Lee, "Fabrication of microcapacitors using conducting polymer micro-electrodes", *J. Power Sources*, vol. 124, pp. 343-350, 2003
- [3] H.J. In, S. Kumar, Y. Shao-Horn, and G. Barbastathis, "Nanostructured Origami™ 3D Fabrication and Assembly of Electrochemical Energy Storage Devices", *Proc 2005 IEEE on Nanotechnology*, Nagoya, Japan, July 2005 pp. 374-377.
- [4] K.H. An, W.S. Kim, Y.S. Park, Y.C. Choi, S.M. Lee, D.C. Chung, D.J. Bae, S.C. Lim, and Y.H. Lee, "Supercapacitors Using Single-Walled Carbon Nanotube Electrodes", *Adv. Mater.*, vol. 13, pp. 497-500, 2001
- [5] V.L. Pushparaj, M.M. Shaijumon, A. Kumar, S. Murugesan, L.J. Ci, R. Vajtai, R.J. Linhardt, O. Nalamasu, and P.M. Ajayan, "Flexible energy storage devices based on nanocomposite paper", *PNAS*, vol. 104, pp. 13574-13577, 2007.
- [6] A.G. Pandolfo and A.F. Hollenkamp, "Carbon properties and their role in supercapacitors", *J. Power Sources*, vol. 157, pp.11-27, 2006
- [7] <http://www.cheaptubes.com/MWNTs.htm>
- [8] H. Zhang, G. Cao, and Y. Yang, "Electrochemical properties of ultra-long, aligned, carbon nanotube array electrode in organic electrolyte", *J. Power Sources*, vol. 172, pp.476-480, 2007
- [9] A.E. Aliev, C. Guthy, M. Zhang, S. Fang, A.A. Zakhidov, J.E. Fischer, and R.H. Baughman, "Thermal transport in MWCNT sheets and yarns", *Carbon*, vol. 45, pp.2880-2888, 2007
- [10] S. Talapatra, S. Kar, S.K. Pal, R. Vajtai, L. Ci, P. Victor, M.M. Shaijumon, S. Kaur, O. Nalamasu and P.M. Ajayan, "Direct growth of aligned carbon nanotubes on bulk metals", *Nature nanotechnology*, vol. 1, pp. 112-116, 2006
- [11] C. Wakai, A. Oleinikova, M. Ott, and H. Weingartner, "How Polar Are Ionic Liquids? Determination of the Static Dielectric Constant of an Imidazolium-based Ionic Liquid by Microwave Dielectric Spectroscopy", *J. Phys. Chem. B*, vol. 109, pp.17028-17030, 2005
- [12] http://www.utexas.edu/research/chemed/lagowski/WSSP/houston_2006_paper_maass_katie.pdf